electron-transfer rate constant is the result of a large difference in structure between the reactant and product of reaction 2. X-ray crystal structures show that the Mn atom residues 0.27 Å above the porphyrin plane in $Mn^{III}(TPP)Cl$[28] versus 0.64 Å in $Mn^{II}(TPP)Cl^-$,[29,22] apparently as a result of unfavorable interaction between the singly occupied metal $d_{x^2-y^2}$ orbital and the pyrrole nitrogens of the porphyrin ring. The significant inner-shell reorganization energy associated with this structural change is expected to result also in a large temperature dependence for the rate of the metal-centered electrode reaction. Table I shows that $k_{s,h}$ for reaction 2 decreases to 7.2×10^{-6} cm s^{-1} at 221 K, whereas reaction 1 retains essentially Nernstian behavior under these conditions.

Similar conclusions are reached regarding electrooxidation and -reduction of the iron(III) porphyrins Fe(TPP)X ($X^- = Br^-$, Cl^-, CH_3O^-). The metal-centered one-electron transfers of these species are quasireversible[16] (Table I) as a consequence of structural changes that include displacement of the Fe atom by an additional ~0.2 Å above the porphyrin plane and extension of the metal–axial ligand bond by ~0.1 Å upon Fe^{III} to Fe^{II} reduction. Although it has not been established that the axial ligand remains bound to the metal after reduction to Fe^{II}, the trend in the measured rate constants ($Br^- > Cl^- > CH_3O^-$) is thought to arise from the fact that the energy required to stretch the metal–axial ligand bond increases with increasing electron donor strength of the axial ligand. The one-electron porphyrin-centered oxidations of Fe(TPP)X exhibit Nernstian behavior within the limits of experimental uncertainty at 298 and 221 K. Correlation of a rapid electrode reaction rate with ring-centered electron transfer is significant particularly in the case of Fe(TPP)Cl oxidation, because the product of this reaction, which was once thought to be an iron(IV) species,[2b] is now definitely characterized as a porphyrin π cation radical.[2d,f] If the electron removed upon Fe(TPP)Cl oxidation had originated from a metal-centered orbital, the structural changes predicted[2d] upon Fe^{III} to Fe^{IV} oxidation would produce a detectably slow electrode reaction.

Another circumstance in which electron transfer at the metal can be distinguished from that at the ring is when the metal undergoes a change in coordination number during an electrode reaction. This behavior is illustrated by electrooxidation of four-coordinate $Co^{II}(TPP)$. Under rigorously noncoordinating conditions Co(TPP) is oxidized to its π cation radical,[4a] whereas in the presence of an intentionally added ligand such as methanol oxidation at the metal precedes that at the ring.[3,30]

$$Co^{II}(TPP) + 2CH_3OH \rightleftharpoons Co^{III}(TPP)(CH_3OH)_2^+ + e^- \quad (3)$$

Figure 2 shows that the metal-centered character of the initial oxidation in the presence of methanol is detectable from its apparent electrode kinetics. The metal-centered oxidation at 0.72 V (eq 3) exhibits sweep-rate-dependent peak potential separations, whereas the porphyrin-centered oxidation at 1.10 V (eq 4) is

$$Co^{III}(TPP)(CH_3OH)_2^+ \rightleftharpoons Co^{III}(TPP^\bullet)(CH_3OH)_2^{2+} + e^- \quad (4)$$

electrochemically reversible. The apparent sluggishness of eq 3 presumably reflects the kinetics of association and dissociation of CH_3OH at the metal center rather than slow electron transfer resulting from a large inner-shell reorganization energy.

In the foregoing examples discrimination between metal- and ring-centered electron transfer on the basis of electrode kinetic behavior is made easily because the structural changes associated with the metal-centered reactions are large. However, in the event of other metal atom coordination geometries and/or spin states smaller changes in structure induced by the change in oxidation state may render the correlation between electron-transfer rate and electron-transfer site less definitive. To test this possibility, we examined the electrode reduction kinetics of four-coordinate $Co^{II}(TPP)$ and the low-spin, six-coordinate complex $Fe^{III}(TPP)(Im)_2^+$.[21]

$$Co^{II}(TPP) + e^- \rightleftharpoons Co^{I}(TPP)^- \quad (5)$$

$$Fe^{III}(TPP)(Im)_2^+ + e^- \rightleftharpoons Fe^{II}(TPP)(Im)_2 \quad (6)$$

In these geometries the metal atom remains essentially in the porphyrin plane and experiences little change in metal–porphyrin and metal–axial ligand distances upon reduction. However, Table I shows that the kinetics of reactions 5 and 6, although more facile than the metal-centered reductions of five-coordinate porphyrins, are less rapid than the essentially reversible porphyrin-centered oxidations. We surmise that either (i) the relatively small structural changes[31] that occur upon reduction of $Co^{II}(TPP)$ and $Fe^{III}(TPP)(Im)_2^+$ still constitute a significant inner-shell barrier to the electrode reaction or (ii) the more highly localized charge resulting from electron transfer at the metal center results in a larger outer-shell barrier.

In summary, the site of electron transfer in metalloporphyrins can be correlated with the heterogeneous rate constant of its electrode reaction in the event that large changes in structure accompany reduction or oxidation of the metal. In these cases, electron transfer at the metal is characterized by rate constants of $k_{s,h} \leq 0.01$ cm s^{-1}, whereas electron transfer at the ring is characterized by apparently reversible electrode kinetics ($k_{s,h} \geq 0.1$ cm s^{-1}). When minimal change in structure accompany electron transfer at the metal, rate constants of intermediate value are observed ($k_{s,h} = 0.01$–0.1 cm s^{-1}) and caution is advised in inferring the site of electron transfer from kinetic measurements in these cases.

Acknowledgment. Support of this research by the National Science Foundation under Grant No. CHE-87-18013 is gratefully acknowledged as are helpful conversations with Professors W. R. Scheidt and C. A. Reed.

(28) Tulinsky, A.; Chen, B. M. L. *J. Am. Chem. Soc.* **1977**, *99*, 3647.
(29) Van Atta, R. B.; Strouse, C. E.; Hanson, L. K.; Valentine, J. S. *J. Am. Chem. Soc.* **1987**, *109*, 1425.
(30) The site of electron transfer in the absence and presence of CH_3OH was confirmed by visible wavelength spectroelectrochemistry. A broad, low-intensity Soret band is observed following one-electron oxidation of $Co^{II}(TPP)$ in carefully purified CH_2Cl_2 whereas a red-shifted Soret band of high intensity is observed in the same experiment in the presence of methanol.
(31) On the basis of X-ray crystallographic information, these changes are estimated to be 0.007 Å in the Co–N_p distance for Co(TPP) reduction[32] and 0.04 Å in the Fe–N_{Im} distance and ≤0.01 Å in the Fe–N_p distance for $Fe(TPP)(Im)_2^+$ reduction.[14,33]
(32) (a) Stevens, E. D. *J. Am. Chem. Soc.* **1981**, *103*, 5087. (b) Doppelt, P.; Fischer, J.; Weiss, R. *Inorg. Chem.* **1984**, *23*, 2958.
(33) (a) Collins, D. M.; Countryman, R.; Hoard, J. L. *J. Am. Chem. Soc.* **1972**, *94*, 2066. (b) Scheidt, W. R.; Osvath, S. R.; Lee, Y. J. *J. Am. Chem. Soc.* **1987**, *109*, 1958.

Department of Chemistry
Purdue University School of Science
Indiana University-Purdue University at Indianapolis
Indianapolis, Indiana 46205

Xi Hai Mu
Franklin A. Schultz*

Received February 21, 1990

Preparation and Characterization of a Layered Molybdenum Phosphate with Mo–Mo Bonds: Structure of $Na_3Mo_2P_2O_{11}(OH)\cdot 2H_2O$

There are a number of layered phosphate structures known for the p-, f-, and d-block elements, such as tin, uranium, titanium, zirconium, and vanadium, many of which are noted for their ion exchange or interlayer ionic mobility.[1] We have recently found a large number of new phosphate structure types, containing mixed octahedral–tetrahedral frameworks, in the molybdenum phosphate system using high-temperature solid-state reactions. Compounds such as $Cs_4Mo_8P_{12}O_{52}$,[2] $Cs_4Mo_{10}P_{18}O_{66}$,[3] and $Cs_3Mo_4P_3O_{16}$[4] were

(1) Clearfield, A. *Chem. Rev.* **1988**, *88*, 125.

0020-1669/90/1329-2879$02.50/0

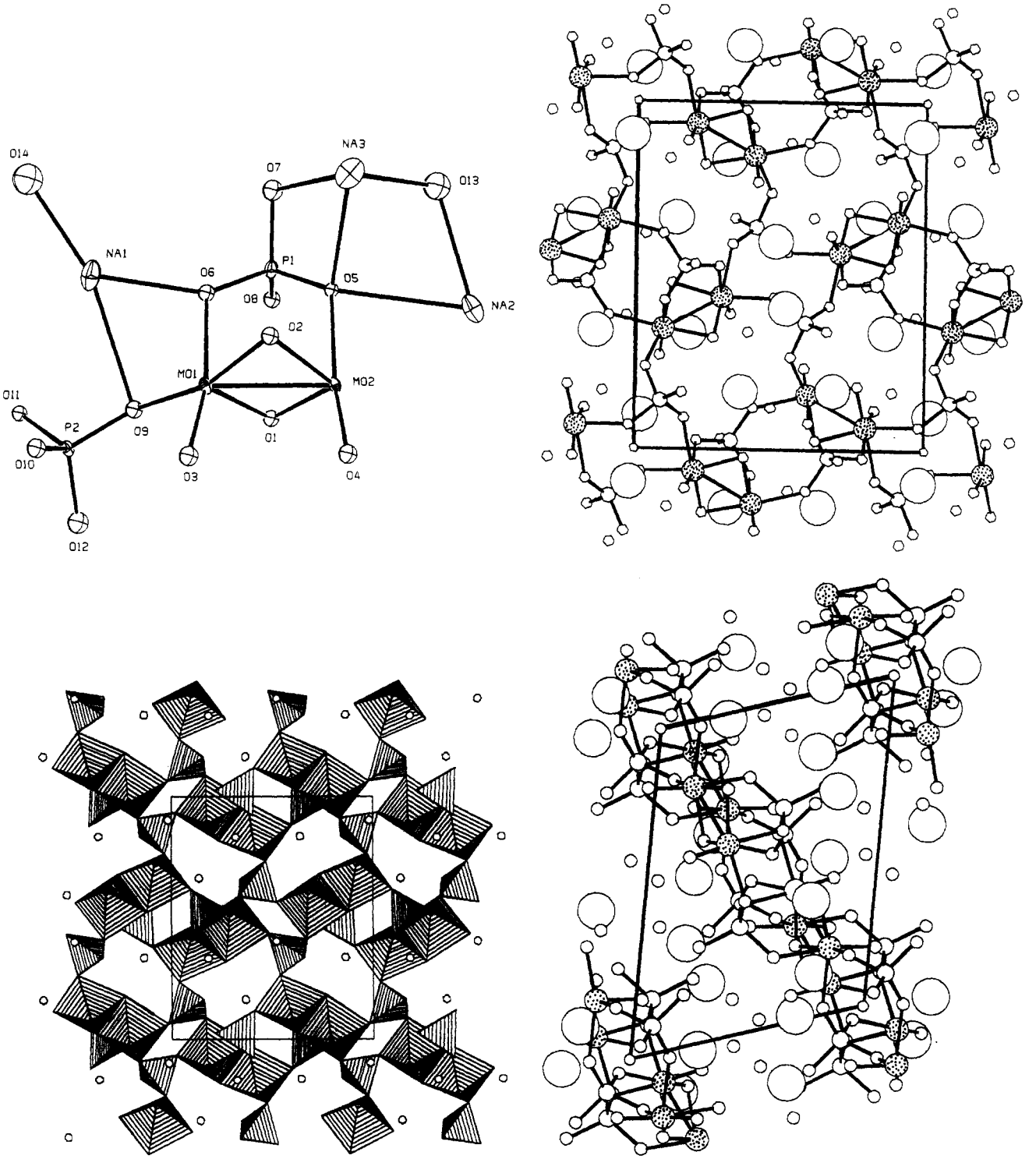

Figure 1. Views of the structure of **1**; (a, upper left) the asymmetric unit showing the anisotropic thermal ellipsoids for the Mo, Na, and P atoms (the O atoms were refined isotropically); (b, upper right) ball-and-stick representation drawn by CHEM-X 89[15] viewed perpendicular to the layer; (c, lower left) a polyhedral representation drawn by STRUPLO 84[16] with the same orientation as in part b; (d, lower right) view parallel to the layers. In parts b and d the large circles are the Na^+ and the smaller circles with no bonds drawn to them are the waters of hydration. The stippled circles are Mo, the four-coordinate circles represent phosphorus, and the remaining circles are O atoms.

isolated. Hydrothermal reactions in the 100–250 °C range have also yielded several novel molybdenum phosphate structures like the large inclusion aggregate $[Na_{14}Mo_{24}P_{17}O_{97}(OH)_{31}]^{6-}$,[5] one-dimensional polymers such as $[(H_3O)_2NaMo_6P_4O_{24}(OH)_7]^{2-}$,[6] and the first transition-metal oxide exhibiting microporosity, $(Me_4N)_{1.3}(H_3O)_{0.7}[Mo_4O_8(PO_4)_2]\cdot 2H_2O$.[7] The only structurally characterized examples of layered molybdenum phosphates are $Cs_2Mo_4P_6O_{26}$,[2] $(Pr_4N)(NH_4)[Mo_4O_8(PO_4)_2]$,[8] and (phenylpyridine)$_2[Mo_4O_8(PO_4)_2]$.[9] We report here the synthesis and structural characterization of a new layered molybdenum phosphate, $Na_3Mo_2P_2O_{11}(OH)\cdot 2H_2O$ (**1**), which contains edge-sharing MoO_6 octahedra with Mo–Mo single bonds.

(2) Lii, K. H.; Haushalter, R. C. *J. Solid State Chem.* **1987**, *69*, 320.
(3) Haushalter, R. C.; Lai, F. W. *J. Solid State Chem.* **1988**, *76*, 218.
(4) Haushalter, R. C. *J. Chem. Soc., Chem. Commun.* **1987**, 374.
(5) Haushalter, R. C.; Lai, F. W. *Angew. Chem.* **1989**, *101*, 802.
(6) Haushalter, R. C.; Lai, F. W. *Inorg. Chem.* **1989**, *28*, 2904.
(7) Haushalter, R. C.; Lai, F. W. *Science* **1989**, *246*, 1289.
(8) Corcoran, E. W. *Inorg. Chem.* **1990**, *29*, 157.
(9) Haushalter, R. C.; Mundi, L. A. Unpublished results.

The hydrothermal reaction of sodium molybdate, molybdenum metal, phosphoric acid, and water in a mole ratio of 6:1.2:6:57 for 90 h at 200 °C gives a 75% yield of dark crystals (pink-brown when crushed) of $Na_3Mo_2P_2O_{11}(OH)\cdot 2H_2O$.[10] The pH of the reaction mixture shortly after mixing, but before heating, is approximately 5. Simulation of the powder X-ray diffraction pattern using the coordinates from the single-crystal X-ray data solution (vide infra) shows that the product is single phase under these conditions.

The structure of **1** was determined from single-crystal X-ray data[11] and represents a new layered structure type. Views of the structure both parallel and perpendicular to the layer are shown in Figure 1. The layers, which run along (101), are composed of edge-sharing MoO_6 octahedra and corner- and edge-sharing phosphate groups. There are half as many MoO_6 dimers as phosphate tetrahedra, which gives a Mo:P ratio of 1, with two crystallographically distinct phosphate groups but only one unique MoO_6 dimer. Each MoO_6 octahedron shares three of its six corners with phosphate groups and two corners with the neighboring edge-sharing octahedron, the sixth corner being a terminal molybdenyl (Mo=O) group. The Mo–Mo distance is 2.575 (2) Å, which corresponds to a metal–metal single bond for Mo, the formulation of which is also supported by the observed diamagnetism of **1**. Each pair of MoO_6 octahedra contacts five different phosphate tetrahedra. Four of these tetrahedra each share a corner with three different dimeric MoO_6 octahedra, while the remaining phosphate group spans, via one of its edges, both oxygen atoms that are trans to the molybdenyl groups of the edge-sharing octahedra and also shares a corner with a different dimer. Both types of phosphate group have a terminal oxygen that protrudes into the interlamellar space. If an oxidation state of 5+ is assigned to the Mo, which is reasonable on the basis of the observed characteristic geometry, the calculated oxidation state from bond strength–bond length equations[12] (which gives 5 ± 0.1), and the observed diamagnetism, then there is only one H^+ per formula unit to be shared between the two terminal phosphate oxygens.[13] Inspection of the P–O bond lengths shows that there is no pronounced lengthening of the terminal P–O bond relative to the bridging oxygens but in phosphoric acid itself the terminal P–O distance is only slightly longer than that of the protonated P–O bonds (0.04–0.06 Å).

In addition to the anionic molybdenum phosphate layer framework, there are three sodium cations and two water molecules per formula unit. There are three crystallographically independent sodium cations, all of which display distorted octahedral coordination, except for Na(2), which has a seventh long Na–O bond at 2.84 Å, by oxygens with Na–O distances ranging from 2.29 to 2.79 Å. Most of these contacts are 2.3–2.5 Å and involve bonds to the phosphate oxygens and the waters of hydration. These water molecules are also involved in an extensive and complicated hydrogen-bonded network to each other and some of the layer oxygen atoms.

While the mechanisms of compound formation in the hydrothermal preparation of this and other of our reduced molybdenum phosphates[5-7] remains obscure, both pH and templating cations have large effects. Compound **1** is the only compound that we have isolated that contains a terminal but unprotonated oxygen atom, which could be due to the higher pH during this reaction. Compound **1** does not form at low pH in the presence of excess phosphoric acid.

The proton and sodium ion mobilities have been studied.[14]

Acknowledgment. We thank D. P. Goshorn for the magnetic susceptibility measurements.

Supplementary Material Available: Tables of experimental crystallographic details, derived coordinates for the atoms, anisotropic thermal parameters for the Mo, P, and Na atoms, intermolecular distances and angles, selected nonbonded contacts, and derived least-squares planes (12 pages); a listing of observed and calculated structure factors (13 pages). Ordering information is given on any current masthead page.

(10) The molybdenum powder should be <2 μm to achieve appreciable reaction rates.

(11) X-ray data for **1** (fw 551.83): monoclinic, space group $P2_1/n$ (No. 14), a = 8.128 (3) Å, b = 13.230 (4) Å, c = 11.441 (2) Å, β = 108.84°, V = 1164.4 (5) Å^3 at 23 °C, Z = 4. The calculated density is 3.15 g·cm^{-3}, λ = 0.710 69 Å, μ = 25.69 cm^{-1}, and transmission coefficients range from 0.84 to 1.00. For 121 variables and 1186 data, R (R_w) = 0.046 (0.051).

(12) Brown, I. D., Wu, K. K. *Acta Crystallogr.* **1976**, *B32*, 1957.

(13) Since the oxidation state of the Mo atoms is 5+ (see text), the extra positive charge must be present as a proton. Since the terminal phosphate oxygen is the most basic site available, it is the most likely site for the protonation. Critical inspection of the bond distances and angles around the phosphate groups and the coordinated Na^+ in question suggests a slight preference for protonation at the O(7) site. We thank a reviewer for pointing this out.

(14) Tsai, M.; Feng, S.; Greenblatt, M.; Haushalter, R. Submitted for publication.

(15) CHEM-X, designed and distributed by Chemical Design Ltd., Mahwah, NJ.

(16) Fischer, R. X. *J. Appl. Crystallogr.* **1985**, *18*, 258.

Exxon Research and Engineering Company
Annandale, New Jersey 08801

Linda A. Mundi
Robert C. Haushalter*

Received February 27, 1990

Iron–Hydroxide Stretching Resonance Raman Bands of a Water-Soluble Sterically Hindered Porphyrin

Resonance Raman (RR) spectroscopy is capable of providing important information about the strength of Fe–ligand bonds in heme proteins via the frequencies of the Fe–ligand stretching vibrational modes.[1] In particular, Fe^{III}–OH stretching RR bands have been reported at 500 cm^{-1} for alkaline horseradish peroxidase[2] and at 495 and 490 cm^{-1} for hydroxo-met hemoglobin[3] and myoglobin.[4] However, to our knowledge, no Fe–OH stretching frequency has been reported for a protein-free hydroxo-heme model complex. A principal reason is that hydroxo–Fe^{III} porphyrins have a strong propensity to condense to μ-oxo dimers in alkaline solution. Steric hindrance can inhibit dimer formation, however, and the mono(hydroxo) adduct of Fe^{III}TMP (TMP = dianion of tetramesitylporphyrin) has been reported.[5] Dimerization is also inhibited for [tetrakis(2-*N*-methylpyridiniumyl)-porphinato]iron(III)[6,7] ($Fe(T(2\text{-}N\text{-}Me)PyP)^{5+}(aq)$) complexes and is likely due to the unfavorable charge interaction as well as steric hindrance. Herein, we report the first observation and assignment of ν(Fe–OH) and ν_{sym}(Fe–$(OH)_2$) stretching bands. We have also demonstrated that the bis(hydroxo) complex constitutes an $S = {}^5/_2$, $S = {}^1/_2$ spin equilibrium that is reminiscent of alkaline met myoglobin. Hence, this water-soluble (porphinato)iron(III) complex is an interesting and pertinent model of the ligand field and Coulombic forces that govern the interplay between structure and reactivity at the prosthetic sites of heme proteins.

In Figure 1 we present isotopic evidence for the presence of two Fe–OH stretching bands in the RR spectrum of the $Fe(T(2\text{-}N\text{-}Me)PyP)^{5+}(aq)$ complex in aqueous carbonate buffer at pH 10.[8] The broad band at 541 cm^{-1} shifts to 514 cm^{-1} in $H_2{}^{18}O$, but *up* to 554 cm^{-1} in ^2H_2O. It is also apparent that the 443-cm^{-1} band is sensitive to both ^2H_2O and $H_2{}^{18}O$, although it is difficult to quantitatively evaluate the actual isotope shift because of spectral complexity. The double band may be due to a Fermi

(1) Spiro, T. G. In *Iron Porphyrins, Part Two*; Lever, A. P. B., Gray, H. B., Eds.; Addison-Wesley: Reading, MA, 1983; Chapter 3.

(2) Sitter, A. J.; Shifflet, J. R.; Terner, J. *J. Biol. Chem.* **1988**, *263*, 13032.

(3) Asher, S. A.; Vickery, L. E.; Schuster, T. M.; Sauer, K. *Biochemistry* **1977**, *16*, 5849.

(4) Debois, A.; Lutz, M.; Banerjee, R. *Biochemistry* **1979**, *18*, 1510.

(5) Cheng, R.-J.; Latos-Grazynski, L.; Balch, A. L. *Inorg. Chem.* **1982**, *21*, 2412.

(6) Kobayashi, N. *Inorg. Chem.* **1985**, *24*, 3324.

(7) Chen, S.-M.; Sun, P.-J.; Su, Y. O. Submitted for publication.

(8) Although the pH transitions are sensitive to the presence of coordinating anions other than hydroxide, the ν(Fe–OH) and ν_{sym}(Fe–$(OH)_2$) stretches are not.

0020-1669/90/1329-2881$02.50/0